


## Article

# Aqueous Biphasic Systems Comprising Natural Organic Acid-Derived Ionic Liquids

Maria V. Quental <sup>†</sup>, Matheus M. Pereira <sup>†</sup> , Francisca A. e Silva, João A. P. Coutinho  and Mara G. Freire <sup>\*</sup> 

CICECO—Aveiro Institute of Materials, Department of Chemistry, University of Aveiro, 3810-193 Aveiro, Portugal; mariajquental@gmail.com (M.V.Q.); matheus.pereira@ua.pt (M.M.P.); francisca.silva@ua.pt (F.A.e.S.); jcoutinho@ua.pt (J.A.P.C.)

\* Correspondence: maragfreire@ua.pt; Tel.: +351 234 370 084

<sup>†</sup> These authors contributed equally to this work.

**Abstract:** Despite the progress achieved by aqueous biphasic systems (ABSs) comprising ionic liquids (ILs) in extracting valuable proteins, the quest for bio-based and protein-friendly ILs continues. To address this need, this work uses natural organic acids as precursors in the synthesis of four ILs, namely tetrabutylammonium formate ( $[N_{4444}][HCOO]$ ), tetrabutylammonium acetate ( $[N_{4444}][CH_3COO]$ ), tetrabutylphosphonium formate ( $[P_{4444}][HCOO]$ ), and tetrabutylphosphonium acetate ( $[P_{4444}][CH_3COO]$ ). It is shown that ABSs can be prepared using all four organic acid-derived ILs paired with the salts potassium phosphate dibasic ( $K_2HPO_4$ ) and tripotassium citrate ( $C_6H_5K_3O_7$ ). According to the ABSs phase diagrams,  $[P_{4444}]$ -based ILs outperform their ammonium congeners in their ability to undergo liquid–liquid demixing in the presence of salts due to their lower hydrogen-bond acidity. However, deviations to the Hofmeister series were detected in the salts' effect, which may be related to the high charge density of the studied IL anions. As a proof of concept for their extraction potential, these ABSs were evaluated in extracting human transferrin, allowing extraction efficiencies of 100% and recovery yields ranging between 86 and 100%. To further disclose the molecular-level mechanisms behind the extraction of human transferrin, molecular docking studies were performed. Overall, the salting-out exerted by the salt is the main mechanism responsible for the complete extraction of human transferrin toward the IL-rich phase, whereas the recovery yield and protein-friendly nature of these systems depend on specific “IL-transferrin” interactions.

**Keywords:** aqueous biphasic systems; ionic liquids; human transferrin; extraction; molecular docking



**Citation:** Quental, M.V.; Pereira, M.M.; Silva, F.A.e.; Coutinho, J.A.P.; Freire, M.G. Aqueous Biphasic Systems Comprising Natural Organic Acid-Derived Ionic Liquids.

*Separations* **2022**, *9*, 46. <https://doi.org/10.3390/separations9020046>

Academic Editor:  
Samuel Carda-Broch

Received: 31 December 2021

Accepted: 2 February 2022

Published: 7 February 2022

**Publisher's Note:** MDPI stays neutral with regard to jurisdictional claims in published maps and institutional affiliations.



**Copyright:** © 2022 by the authors. Licensee MDPI, Basel, Switzerland. This article is an open access article distributed under the terms and conditions of the Creative Commons Attribution (CC BY) license (<https://creativecommons.org/licenses/by/4.0/>).

## 1. Introduction

Aqueous biphasic systems (ABSs) are liquid–liquid systems used as extraction techniques, comprising water as the main constituent and (at least) two-phase splitting promoters such as two polymers or a polymer and a salt [1]. These systems may thus be formed free of volatile organic solvents. If their components are wisely chosen, these systems may be used as low-cost, simple, bio- and eco-friendly extraction platforms [2,3]. More recently, with the adoption of ionic liquids (ILs) as ABSs constituents, the limitations of the narrow hydrophobicity-hydrophilicity range of conventional polymeric systems have been defeated, significantly improving the efficiency and selectivity of many separation processes [4,5]. Known as “designer solvents” or “task-specific solvents”, ILs are organic salts that, through the combination of multiple cations and anions, can be designed to fit the purpose of ABS-mediated extraction processes [5,6]. Given the ILs' ability as stabilizing media for several biomolecules [7–9], IL-based ABSs have been successfully applied in the domain of bioseparations, particularly involving proteins [10]. Imidazolium-based ILs, mostly those carrying fluorinated anions, are among the most widely adopted to formulate ABSs [5,10].

Although less investigated, bio-based ILs may help overcome the high cost of conventional imidazolium-based ILs while improving the green features of this class of solvents [11,12]. Examples of bio-based ILs comprise those based on at least one of the following precursors: choline [13,14], glycine-betaine [15,16], guanidine [17,18], purine and pyrimidine nucleobases [19], carbohydrates [20,21], amino acids [14,22], organic acids [13,23], fatty acids [24,25], and terpenes [26,27]. Thus far, ILs bearing a cholinium cation combined with natural acid-derived anions are the most studied and used as protein-friendly options in IL-based ABSs [28–31]. This work continues the pursuit for cheaper and bio-based ILs to form ABSs using formic and acetic acids as natural ILs' anion precursors. To yield four distinct ILs incorporating organic acid-derived anions, tetrabutylphosphonium and tetrabutylammonium were used as the cations. These cations are among the less costly ILs' cation sources available [32] and confer enough hydrophobicity to the IL to create ABSs with salts [33]. After attesting the ability of synthesized ILs to undergo liquid–liquid demixing in the presence of aqueous solutions of salts ( $K_2HPO_4$  or  $C_6H_5K_3O_7$ ), the resulting ABSs were investigated as simpler and faster paths to extracting valuable proteins. Human transferrin (TF), which plays a central role in iron metabolism, was adopted as a model protein in this work. Transferrin is a single unit glycoprotein comprising 679 amino acid residues and has a molecular weight of ca. 79 kDa [34]. Based on its amino acids sequence, transferrin consists of two homologous regions: the N-terminal (residues 1–336) and C-terminal (residues 337–679) domains, each carrying a metal-binding site [34]. Due to its outstanding biological properties, transferrin currently fits a wide array of applications, namely as an essential ingredient in serum-free cell culture media [35,36], drug and gene delivery [37,38], and as a potential biomarker for several diseases [39,40]. Although transferrin can be obtained from human sources by several methods, most are multi-step dependent or involve complex approaches [41–44]. For instance, methods including salt fractionation, gel filtration chromatography, ion-exchange chromatography, immunoaffinity chromatography, dialysis, and ultrafiltration may need to be combined and it may take up to about 4 days to obtain the purified protein [41,45]. Thereby, there is the need to simplify the purification schemes of transferrin, further reinforcing its relevance as a model protein in the current study.

## 2. Materials and Methods

### 2.1. Materials

For the synthesis of the organic acid-derived ILs, the following precursors were used: tetrabutylphosphonium hydroxide ( $[P_{4444}]OH$ , in water solution at 40 wt.%) and tetrabutylammonium hydroxide ( $[N_{4444}]OH$ , in water solution at 40 wt.%), both from Sigma–Aldrich (Saint Louis, MO, USA); acetic acid glacial (PA) and formic acid (91 wt.%) from Fisher Chemical (Geel, Belgium) and Panreac (Barcelona, Spain), respectively. Methanol (HPLC grade) and acetonitrile (99.9 wt.%) were acquired from VWR (Radnor, PA, USA). The salts used in this work (cf. Figure 1) were potassium phosphate dibasic trihydrate ( $K_2HPO_4 \cdot 3H_2O$ , extra pure) and tripotassium citrate monohydrate ( $C_6H_5K_3O_7 \cdot H_2O$ , 99 wt.%), purchased from GPR Rectapur (VWR, Radnor, PA, USA) and Scharlau (Barcelona, Spain), respectively. Human transferrin (TF) (>98.0 wt.% pure) was purchased from Sigma–Aldrich (Saint Louis, MO, USA). The water used was double distilled, passed across a reverse osmosis system, and further treated with a Milli-Q plus 185 water purification apparatus (Merck, Darmstadt, Germany).

### 2.2. Synthesis of Ionic Liquids

Four ILs were synthesized, namely tetrabutylammonium formate ( $[P_{4444}][HCOO]$ ), tetrabutylphosphonium acetate ( $[P_{4444}][CH_3COO]$ ), tetrabutylammonium formate ( $[N_{4444}][HCOO]$ ), and tetrabutylammonium acetate ( $[N_{4444}][CH_3COO]$ ). Figure 1 depicts their full name, acronym, and chemical structure. These ILs were synthesized by neutralizing  $[P_{4444}]OH$  or  $[N_{4444}]OH$  with the respective organic acids, namely formic and acetic acids. In a typical reaction,  $[P_{4444}]OH$  or  $[N_{4444}]OH$  (40 wt.% in water) and the respective organic acids are mixed at 1:1.1 molar ratio. The reaction mixture was kept at

ambient temperature (25 °C) with continuous stirring for at least 24 h. Water was then removed under reduced pressure at 70 °C. The synthesized ILs were washed with acetonitrile/methanol (1:1, *v:v*) to remove unreacted acids. Excess solvent and water were then removed under reduced pressure using a rotary evaporator (70 °C, 2 h) and under high vacuum (70 °C, 72 h). The purity and structure of the synthesized ILs were verified by  $^1\text{H}$  NMR spectroscopy (Supplementary Materials, Figures S1–S4).

## Ionic liquids

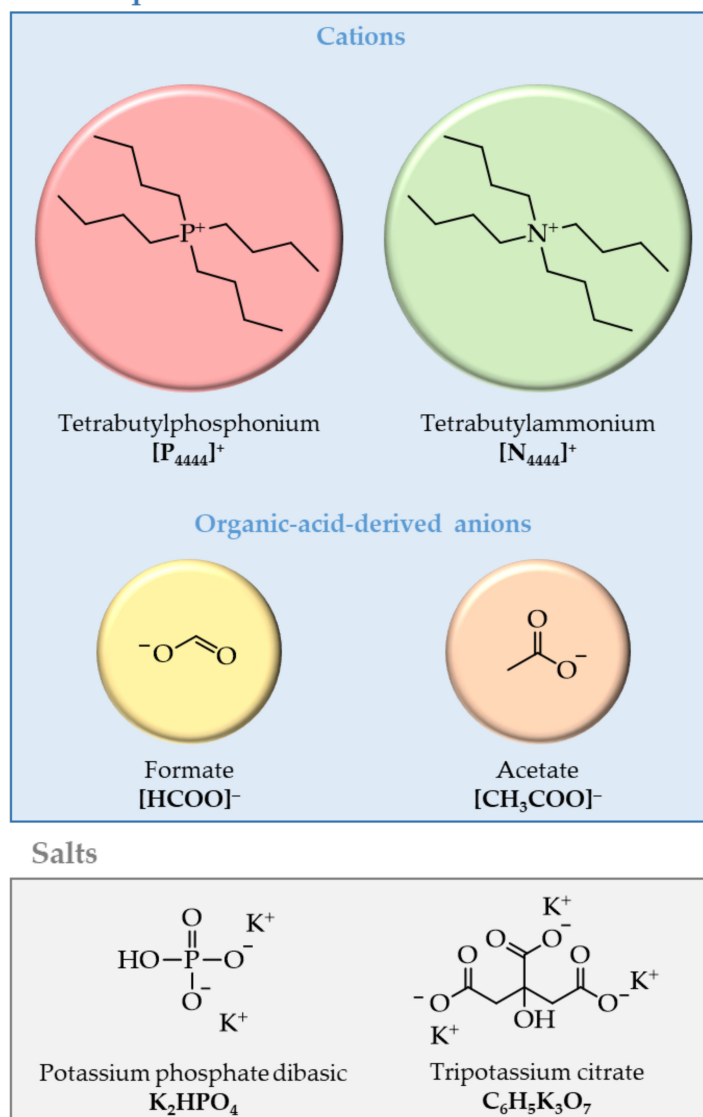


**Figure 1.** Chemical structures, names, and abbreviations of the ABSs constituents studied.

### 2.3. Determination of ABSs Phase Diagrams

The cloud point titration method was used to determine the IL-based ABSs binodal (solubility) curves at (25 ± 1 °C) and atmospheric pressure, following a well-established procedure [46]. Firstly, aqueous solutions of ILs and each salt were prepared gravimetrically at predefined concentrations (i.e., ILs at ca. 50–80 wt.%, K<sub>2</sub>HPO<sub>4</sub> at ca. 40 wt.%, and C<sub>6</sub>H<sub>5</sub>K<sub>3</sub>O<sub>7</sub> at ca. 50 wt.%). The aqueous solution of salt was repetitively added drop by drop to the aqueous solution of IL until a cloudy (biphasic) mixture was detected. Water was then repetitively added drop by drop until a clear and limpid (monophasic) mixture was obtained. These steps were alternately conducted under continuous agitation. After each solution addition, the ternary system compositions of the phase diagram were quantified by weight (within ±10<sup>-4</sup> g). Salt hydrates, namely K<sub>2</sub>HPO<sub>4</sub>·3H<sub>2</sub>O and

$C_6H_5K_3O_7 \cdot H_2O$ , were used. Therefore, the complexed water was regularly considered a portion of the total water in each mixture.

The experimental binodal curves were correlated by the equation proposed by Merchuk et al. [47]. The tie-lines (TLs) and their respective lengths (TLLs) were determined by a gravimetric method developed by the same authors [47]. TLs determination began with the gravimetric preparation of a ternary mixture belonging to the biphasic area of the phase diagram, which was further stirred and centrifuged (30 min, room temperature), allowing for phase separation. Each phase was then separated and weighed, with each TL calculated by the lever-arm rule through the correlation between the IL-rich aqueous phase weight and whole system composition. A more detailed description of the binodal curves correlation and TLs calculation is provided in the literature [46].

#### 2.4. Extraction of Human Transferrin

During the extraction studies, an aqueous solution of human transferrin was prepared at  $0.5 \text{ g} \cdot \text{L}^{-1}$  and used as the water component in the ternary system. A biphasic composition comprising 25 wt.% of IL, 28 wt.% of salt, and 47 wt.% of the transferrin aqueous solution was used. Extraction studies were performed at a pH of  $7.4 \pm 1$ , controlled by adding the respective organic acid precursor (acetic or formic acid) to prepare the IL solutions. The pH of each aqueous phase was measured at  $25 \text{ }^\circ\text{C}$  using an HI 9321 Microprocessor pH meter (HANNA instruments). In both the top and bottom phases, transferrin quantification was conducted by size-exclusion high-performance liquid chromatography (SE-HPLC). A Chromaster HPLC system (VWR Hitachi) equipped with a binary pump, column oven, temperature-controlled auto-sampler, and diode array detector (DAD) was used. The analytical column was a Shodex Protein KW-802.5 ( $8 \text{ mm} \times 300 \text{ mm}$ ). Both the column and autosampler worked at a controlled temperature of  $25 \text{ }^\circ\text{C}$ . The mobile phase was made of a 50 mM phosphate buffer at pH 7.0 with 0.3 M NaCl, which ran in isocratic mode at a flow rate of  $0.5 \text{ mL} \cdot \text{min}^{-1}$ , and the injection volume was 25  $\mu\text{L}$ . The DAD was set at a wavelength of 280 nm. Before injection in the SE-HPLC, each phase was diluted at a 1:10 ( $v/v$ ) ratio in phosphate buffer (50 mM).

Equations 1 and 2 were used to calculate the extraction efficiencies ( $EE_{TF}$ , %) and recovery yields ( $Y_{TF}$ , %) of transferrin, where  $w_{TF}^{IL}$ ,  $w_{TF}^{Salt}$  and  $w_{TF}^{Initial}$  represent the total weight of transferrin in the IL-rich phase, salt-rich phase, and initial mixture, respectively.

$$EE_{TF}, \% = \frac{w_{TF}^{IL}}{w_{TF}^{IL} + w_{TF}^{Salt}} \times 100 \quad (1)$$

$$Y_{TF}, \% = \frac{w_{TF}^{IL}}{w_{TF}^{Initial}} \times 100 \quad (2)$$

#### 2.5. Molecular Docking

The interactions of transferrin with IL cations ( $[N_{4444}]^+$  and  $[P_{4444}]^+$ ) and anions ( $[CH_3COO]^-$  and  $[HCOO]^-$ ) were calculated using AutoDock Vina 1.1.2 [48]. The crystal structure of transferrin (PDB: 3v83) was used in the molecular docking analysis as a receptor. The PDB file was downloaded from the Protein Data bank and uploaded in ProteinPrepare [49]. The pKa calculation was performed at pH 6.5 and pH 8 (average pH of experimentally studied ABSs) without water molecules. AutoDockTools (ADT) [50] was used to prepare the protonated proteins input files. Ligands (ILs ions) 3D atomic coordinates were created using Discovery Studio, v20 (Accelrys, San Diego, CA, USA), and applied to Chem3D-MM2 protocol for energy minimization (Chem3D Ultra, CambridgeSoft Co., Cambridge, MA, USA, 02140). Ligands rigid roots were generated using AutoDockTools (ADT), setting all possible rotatable bonds defined as active by torsions. The grid center at the center of mass ( $x$ -,  $y$ -, and  $z$ -axes) for transferrin was  $-52.411 \times 17.914 \times -30.166$ , respectively. The grid dimension was  $98 \text{ \AA} \times 126 \text{ \AA} \times 112 \text{ \AA}$ . The binding model with the

lowest binding free energy was sought out from nine different conformers for each ligand (IL cations and anions).

### 3. Results and Discussion

#### 3.1. ABSs Phase Diagrams

The potential for natural organic acid-derived ILs to create ABSs was initially evaluated by determining their phase diagrams with  $C_6H_5K_3O_7$  and  $K_2HPO_4$  as the salting-out agents. Four ILs were synthesized (viz.  $[P_{4444}][HCOO]$ ,  $[P_{4444}][CH_3COO]$ ,  $[N_{4444}][HCOO]$  and  $[N_{4444}][CH_3COO]$ ) and the respective binodal curves were determined at 25 °C and atmospheric pressure, and further correlated using the equation proposed by Merchuk et al. [47]. All related data, as well as TLs and TLLs, are provided in Supplementary Materials (Tables S1–S4). Despite the importance of weight percent representations for projecting extraction processes more directly, molality units were used to plot Figures 2 and 3. Molality representations are useful in discussing ABSs formation trends more accurately by excluding any effects derived from the distinct molecular weights of the ILs and salts studied. The experimental binodal data in weight percent reported in Tables S1 and S2 in Supplementary Materials was converted to molality units ( $mol \cdot kg^{-1}$ , moles of IL per kg of salt + water or moles of salt per kg of IL + water) according to the following equation:

$$molality_{IL/salt} \text{ mol} \cdot \text{kg}^{-1} = \frac{\frac{wt.\%_{IL/salt} \times 0.01}{MW_{IL/salt}}}{(100 - wt.\%_{IL/salt}) \times 0.01} \times 1000 \quad (3)$$

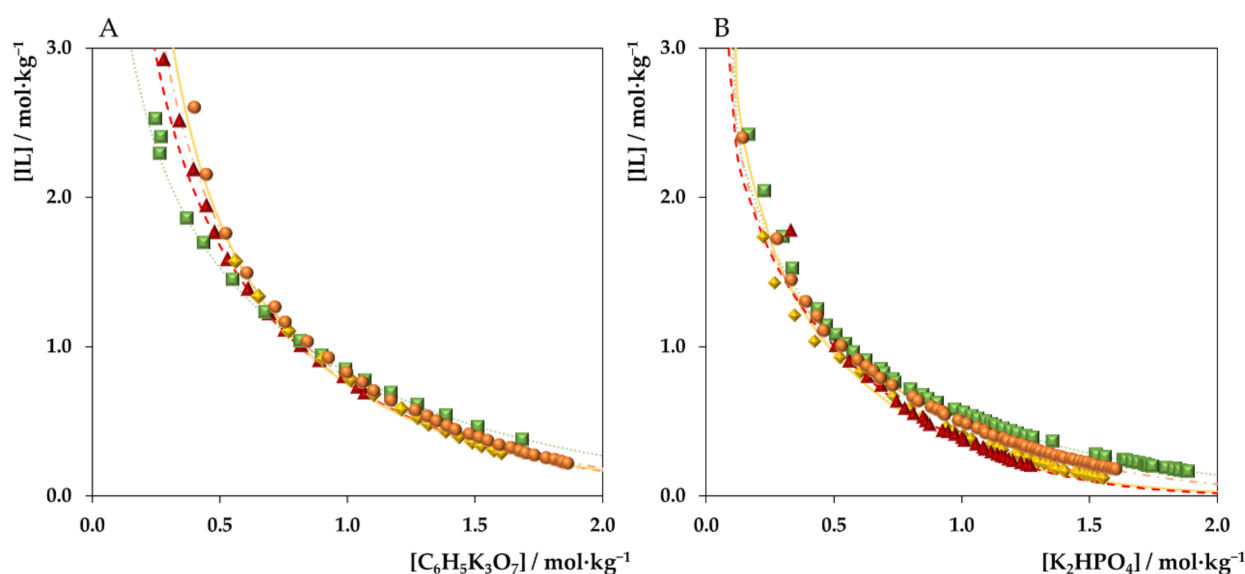


**Figure 2.** Binodal curves of ABSs comprising  $C_6H_5K_3O_7$  (A) or  $K_2HPO_4$  (B) and organic acid-derived ILs at 25 °C and atmospheric pressure:  $[N_{4444}][CH_3COO]$  (■);  $[N_{4444}][HCOO]$  (●);  $[P_{4444}][CH_3COO]$  (◆); and  $[P_{4444}][HCOO]$  (▲).

Figure 2 shows the impact of the IL chemical structure on the formation of ABSs. All  $[N_{4444}]$ - and  $[P_{4444}]$ -based ILs can undergo liquid–liquid demixing in the presence of both salts, exhibiting a similar predisposition to form ABSs. Although binodal curves are somewhat overlaying in the case of  $C_6H_5K_3O_7$ , a more defined trend of ILs' aptitude to form ABSs can be established in the presence of  $K_2HPO_4$  at  $1.0 \text{ mol} \cdot \text{kg}^{-1}$ :  $[P_{4444}][HCOO] > [P_{4444}][CH_3COO] > [N_{4444}][HCOO] > [N_{4444}][CH_3COO]$ . Overall,  $[P_{4444}]$ -based ILs are stronger phase splitting promoters than their  $[N_{4444}]$ -based congeners in the presence of salts, which is a well-documented phenomenon [46]. In turn, ILs bearing the  $[HCOO]^-$  anion appear more susceptible to undergoing two-phase separation than those comprising the  $[CH_3COO]^-$  anion.



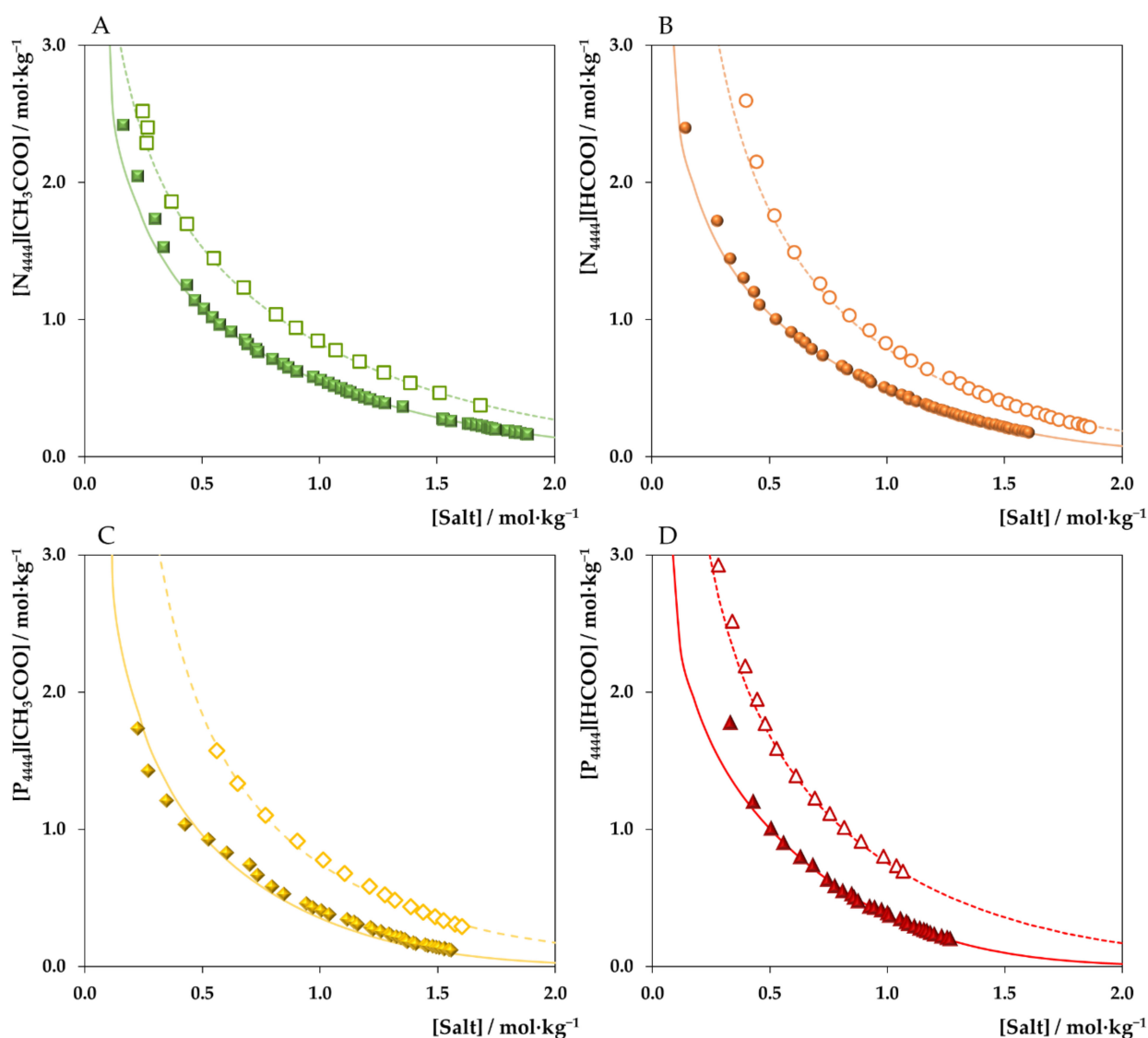


**Figure 3.** Binodal curves of ABSs comprising  $[N_{4444}][CH_3COO]$  (A),  $[N_{4444}][HCOO]$  (B),  $[P_{4444}][CH_3COO]$  (C) and  $[P_{4444}][HCOO]$  (D) and salts at 25 °C and atmospheric pressure:  $K_2HPO_4$  (closed symbols) or  $C_6H_5K_3O_7$  (open symbols).

It was previously shown that the formation of IL-salt-based ABSs correlates well with ILs' hydrogen-bond acidity and basicity [51,52]. That is, ILs' aptitude to behave as hydrogen-bond donors or acceptors governs the molecular mechanisms behind ABS formation involving salts and water. Phosphonium-based ILs are more efficient phase splitting promoters than their ammonium-based counterparts due to their lower hydrogen-bond acidity; thus, they are less prone to form hydrogen bonds with water and more easily salted-out by the salt [52]. On the other hand, ILs bearing anions with high hydrogen-bond basicity, such as the  $[CH_3COO]^-$  anion, are less disposed to form ABSs in the presence of salts [51]. No hydrogen-bond basicity data was found for  $[HCOO]$ -based ILs [51]. Even so, the presence of an extra  $-CH_3$  moiety in  $[CH_3COO]^-$  was expected to enlarge the biphasic zone [53], contrasting the trend observed here. Intricate tendencies in the ABS formation ability of other organic acid-derived ILs have been reported elsewhere [29,54].

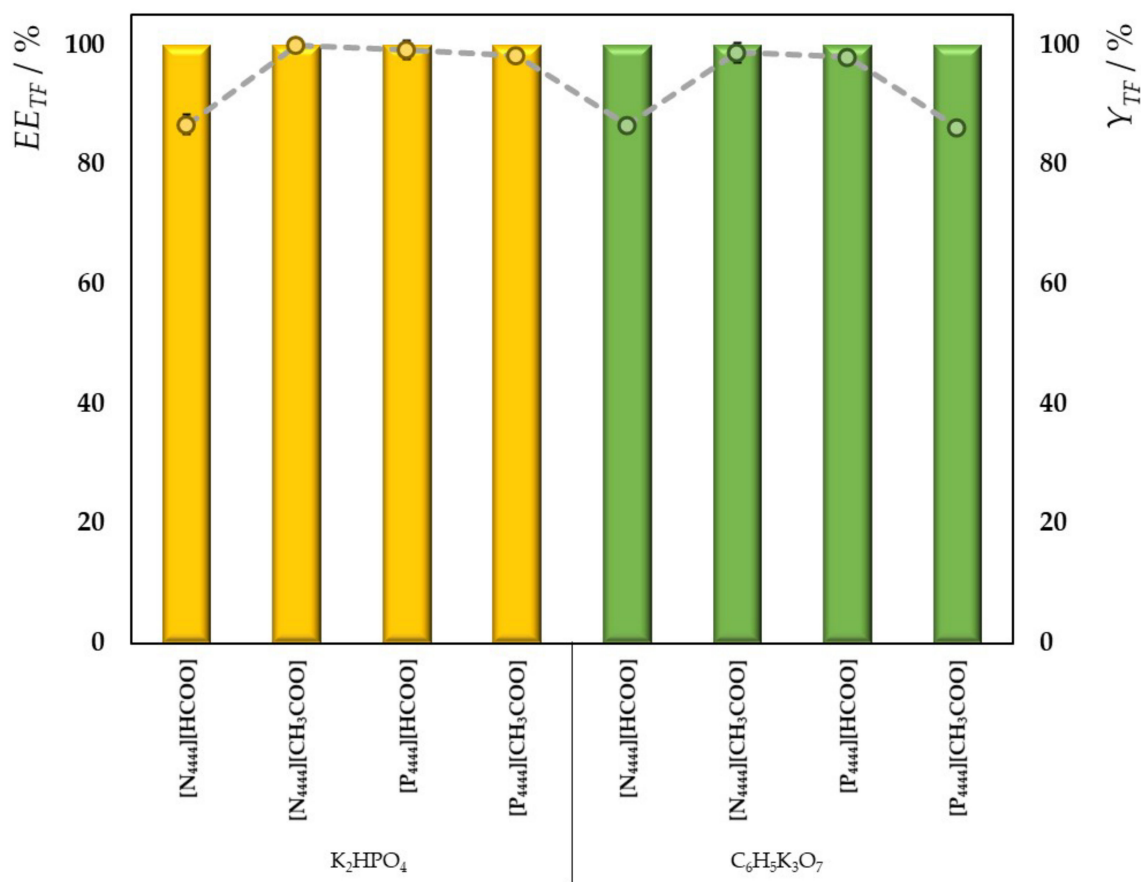
Figure 3 shows the impact of salt on the formation of ABSs.  $K_2HPO_4$  induces the ABS formation more easily in the presence of synthesized ILs than  $C_6H_5K_3O_7$ . This trend is unanticipated considering the Hofmeister series and salt ions' molar entropy of hydration [55]. Accordingly, salts bearing ions of higher valence (e.g.,  $C_6H_5O_7^{3-}$  vs.  $HPO_4^{2-}$ )

are more easily hydrated, thus promoting the generation of IL-based ABSs better [55]. Deviations to the Hofmeister series have also been identified in previous works [51,56], particularly concerning polyvalent ions [57]. In this work, by addressing IL anions with high charge density, it seems that there are competing interactions between the salt anions and IL anions to be hydrated and thus to induce the salting-out or to be salted-out.

### 3.2. Extraction of Transferrin

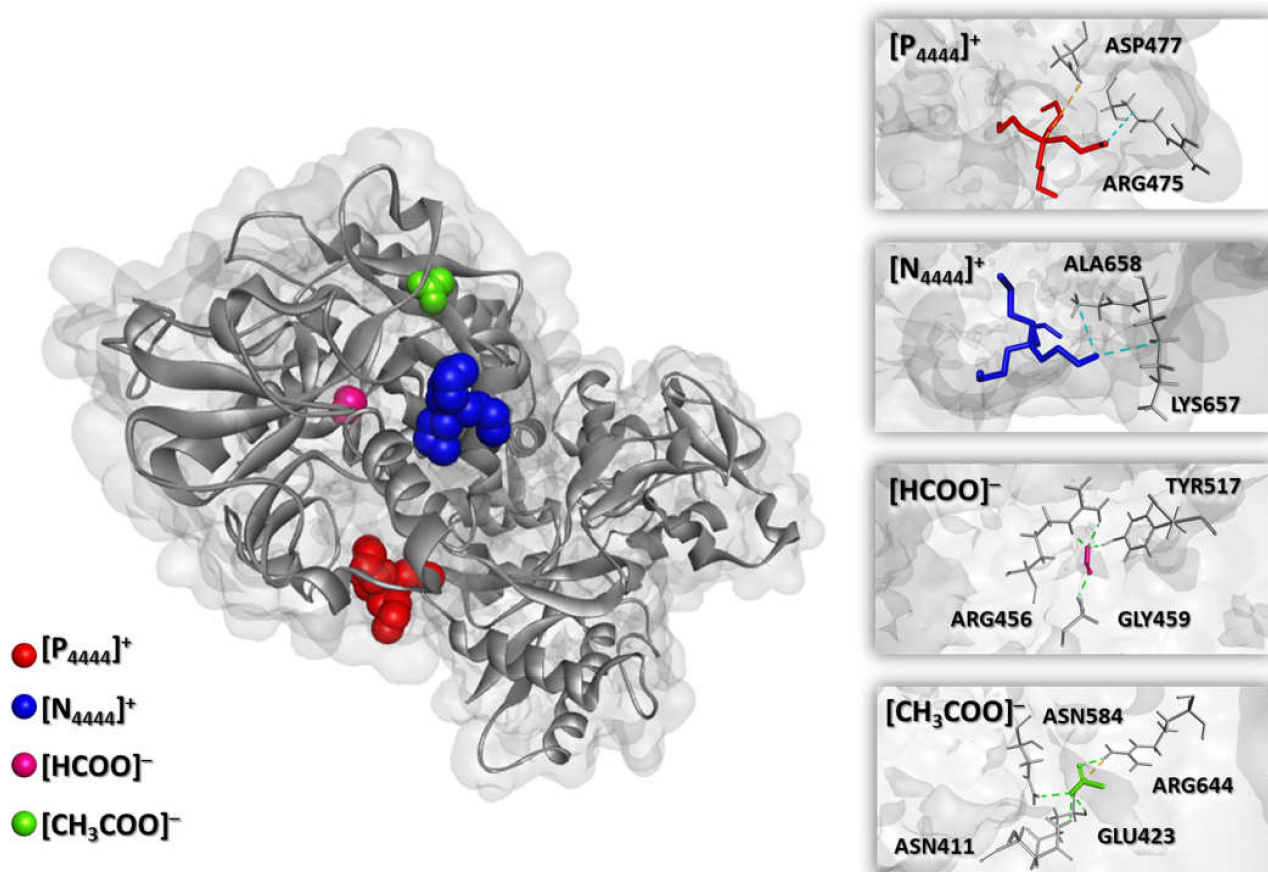
The ABSs proposed herein were investigated as a streamlined extraction platform using human transferrin. To perform the extraction studies, a common mixture point falling within the biphasic region of all ABSs (i.e., 25 wt.% IL + 28 wt.% salt + 47 wt.% aqueous solution containing transferrin) was chosen. Since this method aimed at extracting a labile molecule, namely the protein transferrin, the pH of the extraction medium was controlled at  $7.4 \pm 1$  by initially preparing IL stock solutions with the corresponding precursor organic acid. Detailed pH values are provided in Table S5 of the Supplementary Materials.

Figure 4 shows the extraction efficiencies ( $EE_{TF}$ , %) and recovery yields ( $Y_{TF}$ , %) of transferrin obtained (refer to the Supplementary Materials for numerical data—Table S5). Complete extraction of transferrin toward the IL-rich phase was achieved in one step ( $EE_{TF} = 100\%$ ) with minor losses of protein resulting from precipitation or denaturation phenomena ( $Y_{TF} \geq 86.19 \pm 0.02\%$ ) in all investigated systems. The transferrin partition to the IL-rich phase can be justified based on the salting-out effect produced by the salts; however, differences in the recovery yield may be related to specific “protein-IL” interactions, as discussed below.



**Figure 4.** Extraction efficiencies ( $EE_{TF}$  %, primary scale, bars) and recovery yield ( $Y_{TF}$  %, secondary scale, points) of transferrin achieved with ABSs comprising organic acid-derived ILs and  $K_2HPO_4$  (yellow, left) or  $C_6H_5K_3O_7$  (green, right) at 25 °C and atmospheric pressure.

Molecular docking analysis was performed to shed light on possible “protein-IL” interactions. The docking affinity was calculated for the IL ions ( $[N_{4444}]^+$ ,  $[P_{4444}]^+$ ,  $[CH_3COO]^-$  and  $[HCOO]^-$ ) with transferrin at two protonation states by considering the experimentally measured pH of the systems (Table S5 in Supplementary Materials). The bind poses with the lowest absolute value of affinity ( $\text{kcal}\cdot\text{mol}^{-1}$ ) for transferrin and IL cations/anions are displayed in Figures 5 and 6. The docking bind energies of each IL ion with transferrin, interacting amino acids residues, and type of interaction and geometry distance ( $\text{\AA}$ ) are detailed in Tables S6 and S7 of the Supplementary Materials.



**Figure 5.** Docking pose with the lowest absolute value of affinity ( $\text{kcal}\cdot\text{mol}^{-1}$ ) and interacting amino acids for transferrin (pH 6.5).

Figure 5 shows the bind pose of each IL ion in the transferrin surface at pH 6.5. In  $C_6H_5K_3O_7$ -based and  $K_2HPO_4$ -based systems, the protein is mostly negatively charged (transferrin isoelectric point is around 6 [58]). Therefore, the cation binding affinity to transferrin surfaces derived from electrostatic forces should be higher than the anions studied, as further corroborated by the results obtained (cf. Tables S6 and S7 in Supplementary Materials). The  $[P_{4444}]^+$  cation has a lower bind energy ( $-3.5 \text{ kcal}\cdot\text{mol}^{-1}$ ) than its ammonium congener ( $-4.0 \text{ kcal}\cdot\text{mol}^{-1}$ ). In turn, IL anions have binding affinities with transferrin of  $-3.4$  and  $-3.0 \text{ kcal}\cdot\text{mol}^{-1}$ , for  $[CH_3COO]^-$  and  $[HCOO]^-$ , respectively. According to the bind energy score, the affinity of ILs to interact with transferrin can be rated as follows:  $[N_{4444}][CH_3COO] > [N_{4444}][HCOO] > [P_{4444}][CH_3COO] > [P_{4444}][HCOO]$ . The highest recovery yield ( $Y_{TF} = 98.73 \pm 1.59\%$ ) afforded by  $[N_{4444}][CH_3COO]$  in the presence of  $C_6H_5K_3O_7$  can be attributed to its higher binding energy. Both cations,  $[N_{4444}]^+$  and  $[P_{4444}]^+$ , can also interact through hydrophobic interactions with the protein. Hydrophobic interactions are established with Alanine 658 and Lysine 657 for the former and with Aspartic acid 477 for the latter. In addition, the  $[P_{4444}]^+$  cation is adjacent to Arginine 475, interacting through electrostatic interactions. Both the anions studied are



prone to participate in hydrogen-bonding interactions.  $[\text{CH}_3\text{COO}]^-$  interacts with Arginine 644, Asparagine 411, Glutamic acid 423, and Asparagine 584, whereas  $[\text{HCOO}]^-$  interacts with Arginine 456, Glycine 459, and Tyrosine 517. In addition,  $[\text{CH}_3\text{COO}]^-$  and Arginine 644 establish electrostatic interactions.

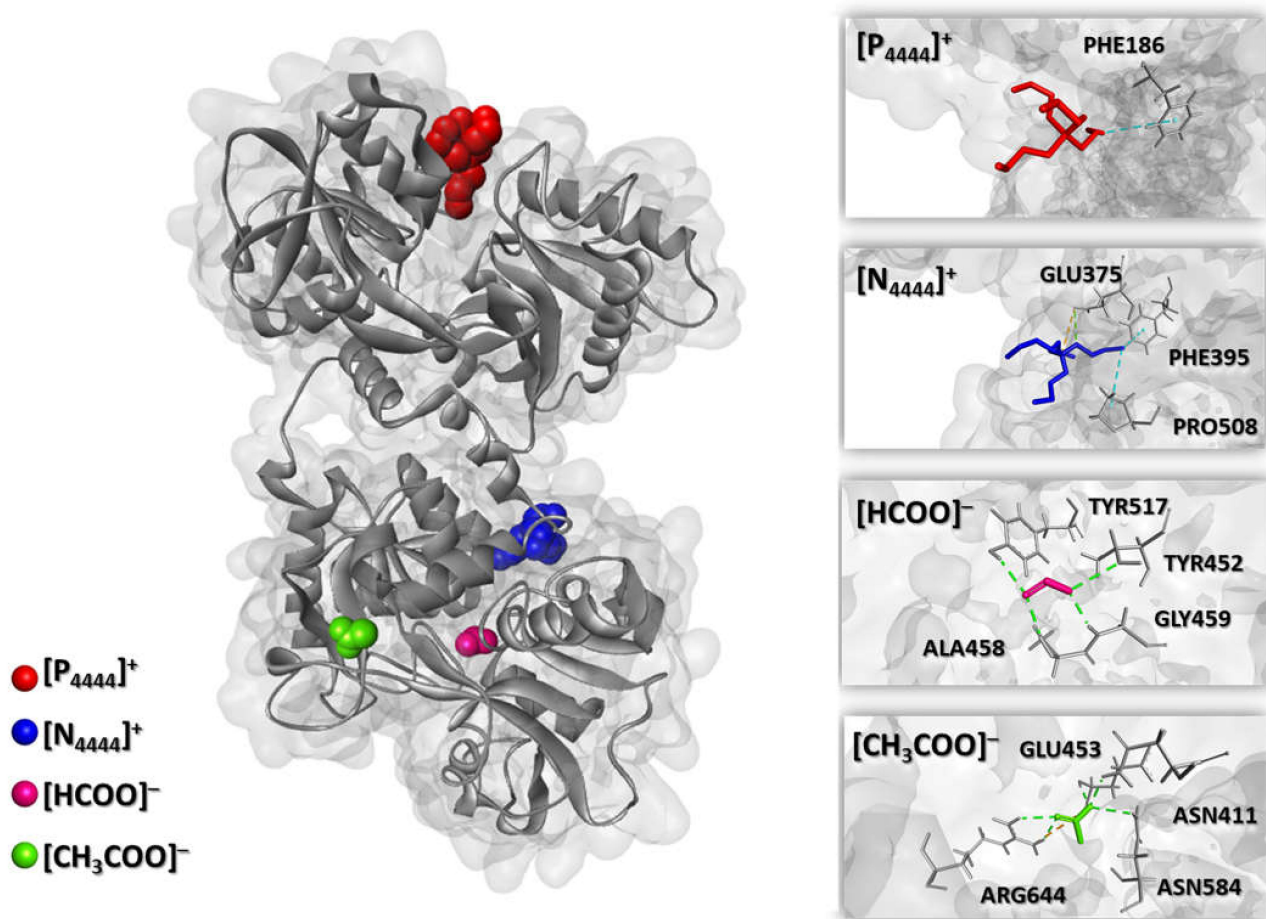


**Figure 6.** Docking pose with the lowest absolute value of affinity ( $\text{kcal}\cdot\text{mol}^{-1}$ ) and interacting amino acids for transferrin (pH 8).

Figure 6 shows the bind poses of each IL ion in the transferrin surface at pH 8. The order of protein-IL docking affinities observed at pH 6.5 also applies for the anions ( $-3.3 \text{ kcal}\cdot\text{mol}^{-1}$  for  $[\text{CH}_3\text{COO}]^-$  and  $-3.1 \text{ kcal}\cdot\text{mol}^{-1}$  for  $[\text{HCOO}]^-$ ). However, it is reversed regarding the cations ( $-3.8 \text{ kcal}\cdot\text{mol}^{-1}$  for  $[\text{N}_{4444}]^+$  and  $-4.0 \text{ kcal}\cdot\text{mol}^{-1}$  for  $[\text{P}_{4444}]^+$ ). Accordingly, the ability of ILs to interact with transferrin at pH 8 follows the order:  $[\text{P}_{4444}][\text{CH}_3\text{COO}] > [\text{P}_{4444}][\text{HCOO}] = [\text{N}_{4444}][\text{CH}_3\text{COO}] > [\text{N}_{4444}][\text{HCOO}]$ . Showing the lowest interaction ability with transferrin,  $[\text{N}_{4444}][\text{HCOO}]$  is the IL leading to the lower recovery yield in ABSs containing  $\text{K}_2\text{HPO}_4$  ( $Y_{TF} = 86.73 \pm 1.57\%$ ). Although transferrin amino acid residues (Phenylalanine 186) only interact with the  $[\text{P}_{4444}]^+$  cation through hydrophobic effects, with  $[\text{N}_{4444}]^+$ , a multitude of interactions occur (viz., hydrophobic effect with Proline 508 and Phenylalanine 395 as well as hydrogen bonds and electrostatic interactions with Glutamic acid 375).  $[\text{HCOO}]^-$  binds to transferrin interacting with Alanine 458, Glycine 459, Tyrosine 517, and Threonine 452 through hydrogen bonds. On the other hand,  $[\text{CH}_3\text{COO}]^-$  is susceptible to interaction by both electrostatic interactions and hydrogen bonding, presenting the same binding sites described at pH 6.5.

Based on the extraction efficiencies obtained (100% for all ABSs studied), it is clear that the partition of transferrin to the IL-rich phase is ruled by a salting-out effect exerted by the salt. However, higher differences were observed in the recovery yields (ranging between 86

and 100%), which seem to result from specific “IL-transferrin” interactions, as unveiled by computational studies, that may reinforce the design of ABSs with a protein-friendly nature.

In a study focused on IL-based ABSs for extracting transferrin, Yee et al. [59] used an ABS comprising 1-butyl-3-methylimidazolium tetrafluoroborate ( $[\text{C}_4\text{C}_1\text{im}][\text{BF}_4]$ ) and sodium phosphate to extract transferrin for point-of-care diagnostic purposes. Although the authors achieved a 20-fold enrichment factor, no extraction efficiencies or recovery yields were reported; therefore, a direct comparison was not possible. Even so,  $[\text{BF}_4]^-$  anion is prone to undergoing hydrolysis yielding hydrofluoric acid [60], being here demonstrated that other IL options exist to extract transferrin.

By focusing on other proteins, Li et al. [29] showed that ABSs comprising organic acid-derived cholinium-based IL and a polymer allow recovery yields between 86.4 and 99.9% of bovine serum albumin, trypsin, papain, and lysozyme. Zafarani-Moatar et al. [31] used ABSs comprising amino acid-derived cholinium-based ILs and polymers to show that extraction efficiencies of bovine serum albumin as high as 85.91% are achievable. With ABSs formed by cholinium-based ILs bearing natural acids as the anions and a polymer, recovery yields of 20 to 100% were obtained for immunoglobulin G by Ramalho et al. [28] and Mondal et al. [30]. Despite their remarkable performance [28–31], most cholinium-based ILs show little to no ability to undergo phase-separation in the presence of most salts [54,61,62], thus limiting their widespread use. In this work, by using  $[\text{P}_{4444}]^+$  or  $[\text{N}_{4444}]^+$  cations in conjugation with organic acid-derived anions, which are more easily salted-out by conventional salts, the toolbox of protein-friendly ABSs is broadened while offering a competitive performance in recovery yield and extraction efficiency.

Finally, it is also worth noting that the synthesis of bio-based ILs comprising organic acids has largely resorted to precursors produced petrochemically rather than naturally (e.g., via fermentation). This strategy is valid to expedite the development of bio-based ILs and their application in separation processes with theoretically transposable outcomes if, for instance, acetic acid—easily produced by the microbial oxidation of ethanol—is considered [63]. Moreover, petrochemically derived organic acids are more easily obtained than their naturally derived equivalents, whose purification is a difficult task [64]. If mixtures of organic acids are used instead of pure compounds, both the IL synthetic pathway and ABS-mediated extraction process may need to be revisited.

#### 4. Conclusions

This work expanded the options available to create protein-friendly IL-based ABSs by using ILs formed by organic acid-derived anions paired with  $[\text{N}_{4444}]^+$  and  $[\text{P}_{4444}]^+$  cations and two salts. Four ILs, viz.  $[\text{N}_{4444}][\text{HCOO}]$ ,  $[\text{N}_{4444}][\text{CH}_3\text{COO}]$ ,  $[\text{P}_{4444}][\text{HCOO}]$  and  $[\text{P}_{4444}][\text{CH}_3\text{COO}]$ , were synthesized via a neutralization reaction and further employed in the development of ABSs. ABSs phase diagrams were established in the presence of  $\text{C}_6\text{H}_5\text{K}_3\text{O}_7$  and  $\text{K}_2\text{HPO}_4$ , allowing to understand the impact of the ILs constituent ions and the salt effect on the two-phase formation. Of all ILs,  $[\text{P}_{4444}][\text{HCOO}]$  and  $[\text{N}_{4444}][\text{CH}_3\text{COO}]$  were identified as the strongest and the weakest phase splitting promoters, respectively. Although the cation effect was governed by the decreased acidity and consequent weaker propensity to establish hydrogen bonds with water, the same does not apply to the impact of the anion, with  $[\text{HCOO}]^-$  outperforming  $[\text{CH}_3\text{COO}]^-$ . Regarding the salts' effect, the formation of ABSs benefited more from the presence of  $\text{K}_2\text{HPO}_4$  than  $\text{C}_6\text{H}_5\text{K}_3\text{O}_7$ , following an opposite trend to the Hofmeister series. This trend may be due to the high charge density of the studied anions, thus improving the competition between the salt and IL anions to be hydrated and to salt-out the competitive ionic species.

Complete extraction ( $EE_{TF} = 100\%$ ) of human transferrin toward the IL-rich phase was achieved with all ABSs, with no major losses of protein ( $86.19 \leq RY_{TF} \leq 100\%$ ). The salting-out effect appear to be mainly responsible for the complete transferrin extraction to the IL-rich phase. By contrast, differences in the recovery yield appear to depend on specific “IL-transferrin” interactions, which in turn provide a protein-friendly environment, as complemented by molecular docking studies.

Overall, the organic acid-derived ILs proposed in this work bestow ABSs with protein-friendly credentials while allowing for high extraction efficiencies and recovery yields. As shown with human transferrin, these systems are expected to contribute significantly to developing streamlined and efficient separation processes for highly valuable proteins. Moreover, to foster the application of ILs derived from natural organic acids in bioseparations, studies involving microbially obtained precursors may be subject to future work.

**Supplementary Materials:** The following supporting information can be downloaded at: <https://www.mdpi.com/article/10.3390/separations9020046/s1>. Figure S1—<sup>1</sup>H NMR spectrum of [P4444][HCOO]. Figure S2—<sup>1</sup>H NMR spectrum of [P4444][CH<sub>3</sub>COO]. Figure S3—<sup>1</sup>H NMR spectrum of [N4444][HCOO]. Figure S4—<sup>1</sup>H NMR spectrum of [N4444][CH<sub>3</sub>COO]. Table S1—Experimental binodal data in weight percent (wt.%) for the ternary systems comprising IL + K<sub>2</sub>HPO<sub>4</sub> + H<sub>2</sub>O at 25 °C and atmospheric pressure. Table S2—Experimental binodal data in weight percent (wt.%) for the ternary systems comprising IL + K<sub>3</sub>C<sub>6</sub>H<sub>5</sub>O<sub>7</sub> + H<sub>2</sub>O at 25 °C and atmospheric pressure. Table S3—A, B, and C parameters of the Merchuk equation and respective correlation coefficients, R<sub>2</sub>, for the ternary systems comprising IL + salt + H<sub>2</sub>O systems at 25 °C and atmospheric pressure. Table S4—Experimental tie-lines (TLs) in weight percent (wt.%) and respective lengths (TLL) for ternary systems comprising IL + salt + H<sub>2</sub>O systems at 25 °C and atmospheric pressure. Initial mixture compositions are represented as [IL]M, and [Salt]M, whereas IL-rich and salt-rich phases compositions are denoted by [IL]IL, [Salt]IL, [IL]Salt, and [Salt]Salt. Table S5—Extraction efficiencies (EETF, %) and recovery yield (YTF, %) of transferrin achieved with ternary systems comprising IL + salt + H<sub>2</sub>O at 25 °C with a controlled pH of  $\approx 7.4 \pm 1$ . Table S6—Docking affinity energy and interacting atoms predicted by AutoDock Vina for transferrin (pH 6.5) + ILs ions. Table S7—Docking affinity energy and interacting atoms predicted by AutoDock Vina for transferrin (pH 8) + ILs ions.

**Author Contributions:** Conceptualization, M.G.F.; methodology, M.V.Q. and M.M.P.; formal analysis, M.V.Q., M.M.P., and F.A.e.S.; investigation, M.V.Q.; writing—original draft preparation, M.V.Q. and M.M.P.; writing—review and editing, F.A.e.S., J.A.P.C., and M.G.F.; visualization, M.M.P. and F.A.e.S.; supervision, J.A.P.C. and M.G.F.; funding acquisition, F.A.e.S. and M.G.F.; project administration, M.G.F. All authors have read and agreed to the published version of the manuscript.

**Funding:** This work was developed within the scope of the project CICECO-Aveiro Institute of Materials, UIDB/50011/2020 & UIDP/50011/2020, financed by national funds through the Portuguese Foundation for Science and Technology/MCTES. This work was funded by national funds (OE) through FCT/MCTES from the project PTDC/EMD-TLM/3253/2020 (ILSurvive), and by FEDER through COMPETE2020—Programa Operacional Competitividade e Internacionalização (POCI), and by national funds (OE) through FCT/MCTES from the project PTDC/BII-BBF/030840/2017 (IL2BioPro). The NMR spectrometers are part of the National NMR Network (PTNMR) and are partially supported by Infrastructure Project N<sup>o</sup> 022161 (cofinanced by FEDER through COMPETE 2020, POCI and PORL, and FCT through PIDDAC). MVQ acknowledges FCT for the PhD grant SFRH/BD/100155/2014. F.A.e.S. acknowledges FCT for the researcher contract CEECIND/03076/2018 under the Scientific Employment Stimulus—Individual Call 2018.

**Institutional Review Board Statement:** Not applicable.

**Informed Consent Statement:** Not applicable.

**Data Availability Statement:** Data is available within the article or Supplementary Materials.

**Conflicts of Interest:** The authors declare no conflict of interest.

## References

1. Albertsson, P.-Å. Partition of Proteins in Liquid Polymer–Polymer Two-Phase Systems. *Nature* **1958**, *182*, 709–711. [[CrossRef](#)]
2. Soares, R.R.G.; Azevedo, A.M.; Van Alstine, J.M.; Aires-Barros, M.R. Partitioning in aqueous two-phase systems: Analysis of strengths, weaknesses, opportunities and threats. *Biotechnol. J.* **2015**, *10*, 1158–1169. [[CrossRef](#)]
3. Iqbal, M.; Tao, Y.; Xie, S.; Zhu, Y.; Chen, D.; Wang, X.; Huang, L.; Peng, D.; Sattar, A.; Shabbir, M.A.B.; et al. Aqueous two-phase system (ATPS): An overview and advances in its applications. *Biol. Proced. Online* **2016**, *18*, 18. [[CrossRef](#)] [[PubMed](#)]
4. Gutowski, K.E.; Broker, G.A.; Willauer, H.D.; Huddleston, J.G.; Swatoski, R.P.; Holbrey, J.D.; Rogers, R.D. Controlling the Aqueous Miscibility of Ionic Liquids: Aqueous Biphasic Systems of Water-Miscible Ionic Liquids and Water-Structuring Salts for Recycle, Metathesis, and Separations. *J. Am. Chem. Soc.* **2003**, *125*, 6632–6633. [[CrossRef](#)] [[PubMed](#)]

5. Basaiahgari, A.; Gardas, R.L. Ionic liquid-based aqueous biphasic systems as sustainable extraction and separation techniques. *Curr. Opin. Green Sustain. Chem.* **2021**, *27*, 100423. [[CrossRef](#)]
6. Welton, T. Ionic liquids: A brief history. *Biophys. Rev.* **2018**, *10*, 691–706. [[CrossRef](#)] [[PubMed](#)]
7. Fujita, K.; Forsyth, M.; MacFarlane, D.R.; Reid, R.W.; Elliott, G.D. Unexpected improvement in stability and utility of cytochrome c by solution in biocompatible ionic liquids. *Biotechnol. Bioeng.* **2006**, *94*, 1209–1213. [[CrossRef](#)]
8. Vijayaraghavan, R.; Izgorodin, A.; Ganesh, V.; Surianarayanan, M.; MacFarlane, D.R. Long-Term Structural and Chemical Stability of DNA in Hydrated Ionic Liquids. *Angew. Chem. Int. Ed.* **2010**, *49*, 1631–1633. [[CrossRef](#)]
9. Mazid, R.R.; Divisekera, U.; Yang, W.; Ranganathan, V.; MacFarlane, D.R.; Cortez-Jugo, C.; Cheng, W. Biological stability and activity of siRNA in ionic liquids. *Chem. Commun.* **2014**, *50*, 13457–13460. [[CrossRef](#)] [[PubMed](#)]
10. Lee, S.Y.; Khoiroh, I.; Ooi, C.W.; Ling, T.C.; Show, P.L. Recent Advances in Protein Extraction Using Ionic Liquid-based Aqueous Two-phase Systems. *Sep. Purif. Rev.* **2017**, *46*, 291–304. [[CrossRef](#)]
11. Gomes, J.M.; Silva, S.S.; Reis, R.L. Biocompatible ionic liquids: Fundamental behaviours and applications. *Chem. Soc. Rev.* **2019**, *48*, 4317–4335. [[CrossRef](#)] [[PubMed](#)]
12. Hulsbosch, J.; De Vos, D.E.; Binnemans, K.; Ameloot, R. Biobased Ionic Liquids: Solvents for a Green Processing Industry? *ACS Sustain. Chem. Eng.* **2016**, *4*, 2917–2931. [[CrossRef](#)]
13. Petkovic, M.; Ferguson, J.L.; Gunaratne, H.Q.N.; Ferreira, R.; Leitão, M.C.; Seddon, K.R.; Rebelo, L.P.N.; Pereira, C.S. Novel biocompatible cholinium-based ionic liquids—toxicity and biodegradability. *Green Chem.* **2010**, *12*, 643–649. [[CrossRef](#)]
14. Le Donne, A.; Bodo, E. Cholinium amino acid-based ionic liquids. *Biophys. Rev.* **2021**, *13*, 147–160. [[CrossRef](#)] [[PubMed](#)]
15. Parajó, J.J.; Macário, I.P.E.; De Gaetano, Y.; Dupont, L.; Salgado, J.; Pereira, J.L.; Gonçalves, F.J.M.; Mohamadou, A.; Ventura, S.P.M. Glycine-betaine-derived ionic liquids: Synthesis, characterization and ecotoxicological evaluation. *Ecotoxicol. Environ. Saf.* **2019**, *184*, 109580. [[CrossRef](#)] [[PubMed](#)]
16. De Gaetano, Y.; Mohamadou, A.; Boudesocque, S.; Hubert, J.; Plantier-Royon, R.; Dupont, L. Ionic liquids derived from esters of Glycine Betaine: Synthesis and characterization. *J. Mol. Liq.* **2015**, *207*, 60–66. [[CrossRef](#)]
17. Pacheco-Fernández, I.; Pino, V.; Ayala, J.H.; Afonso, A.M. Guanidinium ionic liquid-based surfactants as low cytotoxic extractants: Analytical performance in an in-situ dispersive liquid–liquid microextraction method for determining personal care products. *J. Chromatogr. A* **2018**, *1559*, 102–111. [[CrossRef](#)] [[PubMed](#)]
18. Gao, Y.; Arritt, S.W.; Twamley, B.; Shreeve, J.M. Guanidinium-Based Ionic Liquids. *Inorg. Chem.* **2005**, *44*, 1704–1712. [[CrossRef](#)]
19. Gavhane, R.J.; Madkar, K.R.; Kurhe, D.N.; Dagade, D.H. Room Temperature Ionic Liquids from Purine and Pyrimidine Nucleobases. *ChemistrySelect* **2019**, *4*, 5823–5827. [[CrossRef](#)]
20. Poletti, L.; Chiappe, C.; Lay, L.; Pieraccini, D.; Polito, L.; Russo, G. Glucose-derived ionic liquids: Exploring low-cost sources for novel chiral solvents. *Green Chem.* **2007**, *9*, 337. [[CrossRef](#)]
21. Jayachandra, R.; Reddy, S.R. A remarkable chiral recognition of racemic Mosher’s acid salt by naturally derived chiral ionic liquids using 19 F NMR spectroscopy. *RSC Adv.* **2016**, *6*, 39758–39761. [[CrossRef](#)]
22. Egorova, K.S.; Seitkhalieva, M.M.; Posvyatenko, A.V.; Ananikov, V.P. An unexpected increase of toxicity of amino acid-containing ionic liquids. *Toxicol. Res.* **2015**, *4*, 152–159. [[CrossRef](#)]
23. Ferlin, N.; Courty, M.; Gatard, S.; Spulak, M.; Quilty, B.; Beadham, I.; Ghavre, M.; Haiß, A.; Kümmerer, K.; Gathergood, N.; et al. Biomass derived ionic liquids: Synthesis from natural organic acids, characterization, toxicity, biodegradation and use as solvents for catalytic hydrogenation processes. *Tetrahedron* **2013**, *69*, 6150–6161. [[CrossRef](#)]
24. Kwan, M.-L.; Mirjafari, A.; McCabe, J.R.; O’Brien, R.A.; Essi, D.F.; Baum, L.; West, K.N.; Davis, J.H. Synthesis and thermophysical properties of ionic liquids: Cyclopropyl moieties versus olefins as Tm-reducing elements in lipid-inspired ionic liquids. *Tetrahedron Lett.* **2013**, *54*, 12–14. [[CrossRef](#)]
25. Uddin, S.; Chowdhury, M.R.; Wakabayashi, R.; Kamiya, N.; Moniruzzaman, M.; Goto, M. Lipid based biocompatible ionic liquids: Synthesis, characterization and biocompatibility evaluation. *Chem. Commun.* **2020**, *56*, 13756–13759. [[CrossRef](#)] [[PubMed](#)]
26. Feder-Kubis, J.; Wnętrzak, A.; Chachaj-Brekiesz, A. Terpene-Based Ionic Liquids from Natural Renewable Sources as Selective Agents in Antifungal Therapy. *ACS Biomater. Sci. Eng.* **2020**, *6*, 3832–3842. [[CrossRef](#)] [[PubMed](#)]
27. Feder-Kubis, J.; Zabielska-Matejuk, J.; Stangierska, A.; Przybylski, P.; Jacquemin, J.; Geppert-Rybczyńska, M. Toward Designing “Sweet” Ionic Liquids Containing a Natural Terpene Moiety as Effective Wood Preservatives. *ACS Sustain. Chem. Eng.* **2019**, *7*, 15628–15639. [[CrossRef](#)]
28. Ramalho, C.C.; Neves, C.M.S.S.; Quental, M.V.; Coutinho, J.A.P.; Freire, M.G. Separation of immunoglobulin G using aqueous biphasic systems composed of cholinium-based ionic liquids and poly (propylene glycol). *J. Chem. Technol. Biotechnol.* **2018**, *93*, 1931–1939. [[CrossRef](#)] [[PubMed](#)]
29. Li, Z.; Liu, X.; Pei, Y.; Wang, J.; He, M. Design of environmentally friendly ionic liquid aqueous two-phase systems for the efficient and high activity extraction of proteins. *Green Chem.* **2012**, *14*, 2941. [[CrossRef](#)]
30. Mondal, D.; Sharma, M.; Quental, M.V.; Tavares, A.P.M.; Prasad, K.; Freire, M.G. Suitability of bio-based ionic liquids for the extraction and purification of IgG antibodies. *Green Chem.* **2016**, *18*, 6071–6081. [[CrossRef](#)]
31. Zafarani-Moattar, M.T.; Shekaari, H.; Jafari, P. Design of Novel Biocompatible and Green Aqueous two-Phase Systems containing Cholinium L-alaninate ionic liquid and polyethylene glycol di-methyl ether 250 or polypropylene glycol 400 for separation of bovine serum albumin (BSA). *J. Mol. Liq.* **2018**, *254*, 322–332. [[CrossRef](#)]



32. Passos, H.; Freire, M.G.; Coutinho, J.A.P. Ionic liquid solutions as extractive solvents for value-added compounds from biomass. *Green Chem.* **2014**, *16*, 4786–4815. [[CrossRef](#)]
33. Bridges, N.J.; Gutowski, K.E.; Rogers, R.D. Investigation of aqueous biphasic systems formed from solutions of chaotropic salts with kosmotropic salts (salt–salt ABS). *Green Chem.* **2007**, *9*, 177–183. [[CrossRef](#)]
34. Gomme, P.T.; McCann, K.B.; Bertolini, J. Transferrin: Structure, function and potential therapeutic actions. *Drug Discov. Today* **2005**, *10*, 267–273. [[CrossRef](#)]
35. Barnes, D.; Sato, G. Serum-free cell culture: A unifying approach. *Cell* **1980**, *22*, 649–655. [[CrossRef](#)]
36. Laskey, J.; Webb, I.; Schulman, H.M.; Ponka, P. Evidence that transferrin supports cell proliferation by supplying iron for DNA synthesis. *Exp. Cell Res.* **1988**, *176*, 87–95. [[CrossRef](#)]
37. Bai, Y.; Ann, D.K.; Shen, W.-C. Recombinant granulocyte colony-stimulating factor-transferrin fusion protein as an oral myelopoietic agent. *Proc. Natl. Acad. Sci. USA* **2005**, *102*, 7292–7296. [[CrossRef](#)]
38. Huang, R.-Q.; Qu, Y.-H.; Ke, W.-L.; Zhu, J.-H.; Pei, Y.-Y.; Jiang, C. Efficient gene delivery targeted to the brain using a transferrin-conjugated polyethyleneglycol-modified polyamidoamine dendrimer. *FASEB J.* **2007**, *21*, 1117–1125. [[CrossRef](#)]
39. Hoshi, K.; Ito, H.; Abe, E.; Fuwa, T.J.; Kanno, M.; Murakami, Y.; Abe, M.; Murakami, T.; Yoshihara, A.; Ugawa, Y.; et al. Transferrin Biosynthesized in the Brain Is a Novel Biomarker for Alzheimer’s Disease. *Metabolites* **2021**, *11*, 616. [[CrossRef](#)] [[PubMed](#)]
40. Atallah, G.A.; Abd Aziz, N.H.; Teik, C.K.; Shafiee, M.N.; Kampan, N.C. New Predictive Biomarkers for Ovarian Cancer. *Diagnostics* **2021**, *11*, 465. [[CrossRef](#)] [[PubMed](#)]
41. Von Bonsdorff, L.; Tölö, H.; Lindeberg, E.; Nyman, T.; Harju, A.; Parkkinen, J. Development of a Pharmaceutical Apotransferrin Product for Iron Binding Therapy. *Biologicals* **2001**, *29*, 27–37. [[CrossRef](#)] [[PubMed](#)]
42. Rivat, C.; Sertillanges, P.; Patin, E.; Stoltz, J.F. Single-step method for purification of human transferrin from a by-product of chromatographic fractionation of plasma. *J. Chromatogr. B Biomed. Sci. Appl.* **1992**, *576*, 71–77. [[CrossRef](#)]
43. McCann, K.B.; Hughes, B.; Wu, J.; Bertolini, J.; Gomme, P.T. Purification of transferrin from Cohn supernatant I using ion-exchange chromatography. *Biotechnol. Appl. Biochem.* **2005**, *42*, 211. [[CrossRef](#)] [[PubMed](#)]
44. Inman, J.K.; Coryell, F.C.; McCall, K.B.; Sgouris, J.T.; Anderson, H.D. A Large-Scale Method for the Purification of Human Transferrin. *Vox Sang.* **1961**, *6*, 34–52. [[CrossRef](#)] [[PubMed](#)]
45. Welch, S. *Transferrin: The Iron Carrier*; CRC Press, Inc.: Boca Raton, FL, USA, 1992; ISBN 978-0849367939.
46. Passos, H.; Ferreira, A.R.; Cláudio, A.F.M.; Coutinho, J.A.P.; Freire, M.G. Characterization of aqueous biphasic systems composed of ionic liquids and a citrate-based biodegradable salt. *Biochem. Eng. J.* **2012**, *67*, 68–76. [[CrossRef](#)]
47. Merchuk, J.C.; Andrews, B.A.; Asenjo, J.A. Aqueous two-phase systems for protein separation studies on phase inversion. *J. Chromatogr. B Biomed. Appl.* **1998**, *711*, 285–293. [[CrossRef](#)]
48. Trott, O.; Olson, A.J. AutoDock Vina: Improving the speed and accuracy of docking with a new scoring function, efficient optimization, and multithreading. *J. Comput. Chem.* **2010**, *31*, 455–461. [[CrossRef](#)] [[PubMed](#)]
49. Martínez-Rosell, G.; Giorgino, T.; De Fabritiis, G. PlayMolecule ProteinPrepare: A Web Application for Protein Preparation for Molecular Dynamics Simulations. *J. Chem. Inf. Model.* **2017**, *57*, 1511–1516. [[CrossRef](#)]
50. Morris, G.M.; Huey, R.; Lindstrom, W.; Sanner, M.F.; Belew, R.K.; Goodsell, D.S.; Olson, A.J. AutoDock4 and AutoDockTools4: Automated docking with selective receptor flexibility. *J. Comput. Chem.* **2009**, *30*, 2785–2791. [[CrossRef](#)] [[PubMed](#)]
51. Passos, H.; Dinis, T.B.V.; Cláudio, A.F.M.; Freire, M.G.; Coutinho, J.A.P. Hydrogen bond basicity of ionic liquids and molar entropy of hydration of salts as major descriptors in the formation of aqueous biphasic systems. *Phys. Chem. Chem. Phys.* **2018**, *20*, 14234–14241. [[CrossRef](#)]
52. Kurnia, K.A.; Lima, F.; Cláudio, A.F.M.; Coutinho, J.A.P.; Freire, M.G. Hydrogen-bond acidity of ionic liquids: An extended scale. *Phys. Chem. Chem. Phys.* **2015**, *17*, 18980–18990. [[CrossRef](#)] [[PubMed](#)]
53. Ding, X.; Wang, Y.; Zeng, Q.; Chen, J.; Huang, Y.; Xu, K. Design of functional guanidinium ionic liquid aqueous two-phase systems for the efficient purification of protein. *Anal. Chim. Acta* **2014**, *815*, 22–32. [[CrossRef](#)] [[PubMed](#)]
54. Berton, P.; Tian, H.; Rogers, R.D. Phase Behavior of Aqueous Biphasic Systems with Choline Alkanoate Ionic Liquids and Phosphate Solutions: The Influence of pH. *Molecules* **2021**, *26*, 1702. [[CrossRef](#)]
55. Shahriari, S.; Neves, C.M.S.S.; Freire, M.G.; Coutinho, J.A.P. Role of the Hofmeister Series in the Formation of Ionic-Liquid-Based Aqueous Biphasic Systems. *J. Phys. Chem. B* **2012**, *116*, 7252–7258. [[CrossRef](#)] [[PubMed](#)]
56. Chen, Y.; Liang, X.; Woodley, J.M.; Kontogeorgis, G.M. Modelling study on phase equilibria behavior of ionic liquid-based aqueous biphasic systems. *Chem. Eng. Sci.* **2022**, *247*, 116904. [[CrossRef](#)]
57. Kurnia, K.A.; Freire, M.G.; Coutinho, J.A.P. Effect of Polyvalent Ions in the Formation of Ionic-Liquid-Based Aqueous Biphasic Systems. *J. Phys. Chem. B* **2014**, *118*, 297–308. [[CrossRef](#)]
58. Takátsy, A.; Hodrea, J.; Majdik, C.; Dan Irímie, F.; Kilár, F. Role of chemical structure in molecular recognition by transferrin. *J. Mol. Recognit.* **2006**, *19*, 270–274. [[CrossRef](#)]
59. Yee, M.F.; Emmel, G.N.; Yang, E.J.; Lee, E.; Paek, J.H.; Wu, B.M.; Kamei, D.T. Ionic Liquid Aqueous Two-Phase Systems for the Enhanced Paper-Based Detection of Transferrin and *Escherichia coli*. *Front. Chem.* **2018**, *6*, 486. [[CrossRef](#)]
60. Freire, M.G.; Neves, C.M.S.S.; Marrucho, I.M.; Coutinho, J.A.P.; Fernandes, A.M. Hydrolysis of Tetrafluoroborate and Hexafluorophosphate Counter Ions in Imidazolium-Based Ionic Liquids. *J. Phys. Chem. A* **2010**, *114*, 3744–3749. [[CrossRef](#)]
61. Basaiahgari, A.; Priyanka, V.P.; Ijardar, S.P.; Gardas, R.L. Aqueous biphasic systems of amino acid-based ionic liquids: Evaluation of phase behavior and extraction capability for caffeine. *Fluid Phase Equilib.* **2020**, *506*, 112373. [[CrossRef](#)]



62. Tian, H.; Berton, P.; Rogers, R.D. Choline-based aqueous biphasic systems: Overview of applications. *Fluid Phase Equilib.* **2019**, *502*, 112258. [[CrossRef](#)]
63. Gomes, R.J.; Borges, M.F.; Rosa, M.F.; Castro-Gómez, R.J.H.; Spinosa, W.A. Acetic Acid Bacteria in the Food Industry: Systematics, Characteristics and Applications. *Food Technol. Biotechnol.* **2018**, *56*, 139. [[CrossRef](#)] [[PubMed](#)]
64. Morales-Vera, R.; Crawford, J.; Dou, C.; Bura, R.; Gustafson, R. Techno-Economic Analysis of Producing Glacial Acetic Acid from Poplar Biomass via Bioconversion. *Molecules* **2020**, *25*, 4328. [[CrossRef](#)] [[PubMed](#)]